

Localized charged-neutral fluctuations in 158A GeV Pb+Pb collisions

M. M. Aggarwal,¹ A. Agnihotri,² Z. Ahammed,³ A. L. S. Angelis,⁴ V. Antonenko,⁵ V. Arefiev,⁶ V. Astakhov,⁶ V. Avdeitchikov,⁶ T. C. Awes,⁷ P. V. K. S. Baba,⁸ S. K. Badyal,⁸ C. Barlag,⁹ S. Bathe,⁹ B. Batiounia,⁶ T. Bernier,¹⁰ K. B. Bhalla,² V. S. Bhatia,¹ C. Blume,⁹ R. Bock,¹¹ E.-M. Bohne,⁹ Z. Bőröcz,⁹ D. Bucher,⁹ A. Buijs,¹² H. Büsching,⁹ L. Carlen,¹³ V. Chalyshev,⁶ S. Chattopadhyay,³ R. Cherbachev,⁵ T. Chujo,¹⁴ A. Claussen,⁹ A. C. Das,³ M. P. Decowski,¹⁸ H. Delagrangé,¹⁰ V. Djordjadze,⁶ P. Donni,⁴ I. Doubrovik,⁵ A. K. Dubey,¹⁹ S. Dutt,⁸ M. R. Dutta Majumdar,³ K. El Chenawi,¹³ S. Eliseev,¹⁵ K. Enosawa,¹⁴ P. Foka,⁴ S. Fokin,⁵ M. S. Ganti,³ S. Garpman,¹³ O. Gavrishchuk,⁶ F. J. M. Geurts,¹² T. K. Ghosh,¹⁶ R. Glasow,⁹ S. K. Gupta,² B. Guskov,⁶ H. Å. Gustafsson,¹³ H. H. Gutbrod,¹⁰ R. Higuchi,¹⁴ I. Hrivnacova,¹⁵ M. Ippolitov,⁵ H. Kalechofsky,⁴ R. Kamermans,¹² K.-H. Kampert,⁹ K. Karadjev,⁵ K. Karpio,¹⁷ S. Kato,¹⁴ S. Kees,⁹ C. Klein-Bösing,⁹ S. Knoche,⁹ B. W. Kolb,¹¹ I. Kosarev,⁶ I. Koutcheryaev,⁵ T. Krümpel,⁹ A. Kugler,¹⁵ P. Kulinich,¹⁸ M. Kurata,¹⁴ K. Kurita,¹⁴ N. Kuzmin,⁶ I. Langbein,¹¹ A. Lebedev,⁵ Y. Y. Lee,¹¹ H. Löhner,¹⁶ L. Luquin,¹⁰ D. P. Mahapatra,¹⁹ V. Manko,⁵ M. Martin,⁴ G. Martínez,¹⁰ A. Maximov,⁶ G. Mgebrichvili,⁵ Y. Miake,¹⁴ Md. F. Mir,⁸ G. C. Mishra,¹⁹ Y. Miyamoto,¹⁴ B. Mohanty,¹⁹ M.-J. Mora,¹⁰ D. Morrison,²⁰ D. S. Mukhopadhyay,³ H. Naef,⁴ B. K. Nandi,¹⁹ S. K. Nayak,¹⁰ T. K. Nayak,³ S. Neumaier,¹¹ A. Nianine,⁵ V. Nikitine,⁶ S. Nikolaev,⁵ P. Nilsson,¹³ S. Nishimura,¹⁴ P. Nomokonov,⁶ J. Nystrand,¹³ F. E. Obenshain,²⁰ A. Oskarsson,¹³ I. Otterlund,¹³ M. Pachr,¹⁵ S. Pavliouk,⁶ T. Peitzmann,⁹ V. Petracek,¹⁵ W. Pinganaud,¹⁰ F. Plasil,⁷ U. v. Poblitzki,⁹ M. L. Purschke,¹¹ J. Rak,¹⁵ R. Raniwala,² S. Raniwala,² V. S. Ramamurthy,¹⁹ N. K. Rao,⁸ F. Retiere,¹⁰ K. Reygers,⁹ G. Roland,¹⁸ L. Rosselet,⁴ I. Roufanov,⁶ C. Roy,¹⁰ J. M. Rubio,⁴ H. Sako,¹⁴ S. S. Sambyal,⁸ R. Santo,⁹ S. Sato,¹⁴ H. Schlagheck,⁹ H.-R. Schmidt,¹¹ Y. Schutz,¹⁰ G. Shabratova,⁶ T. H. Shah,⁸ I. Sibiriak,⁵ T. Siemiarczuk,¹⁷ D. Silvermyr,¹³ B. C. Sinha,³ N. Slavine,⁶ K. Söderström,¹³ N. Solomey,⁴ G. Sood,¹ S. P. Sørensen,^{7,20} P. Stankus,⁷ G. Stefanek,¹⁷ P. Steinberg,¹⁸ E. Stenlund,¹³ D. Stüken,⁹ M. Sumera,¹⁵ T. Svensson,¹³ M. D. Trivedi,³ A. Tsvetkov,⁵ L. Tykarski,¹⁷ J. Urbahn,¹¹ E. C. v. d. Pijll,¹² N. v. Eijndhoven,¹² G. J. v. Nieuwenhuizen,¹⁸ A. Vinogradov,⁵ Y. P. Viyogi,³ A. Vodopianov,⁶ S. Vörös,⁴ B. Wysłouch,¹⁸ K. Yagi,¹⁴ Y. Yokota,¹⁴ and G. R. Young⁷

(WA98 Collaboration)

¹University of Panjab, Chandigarh 160 014, India

²University of Rajasthan, Jaipur 302 004, Rajasthan, India

³Variable Energy Cyclotron Centre, Calcutta 700 064, India

⁴University of Geneva, CH-1211 Geneva 4, Switzerland

⁵RRC “Kurchatov Institute,” RU-123182 Moscow, Russia

⁶Joint Institute for Nuclear Research, RU-141980 Dubna, Russia

⁷Oak Ridge National Laboratory, Oak Ridge, Tennessee 37831-6372

⁸University of Jammu, Jammu 180 001, India

⁹University of Münster, D-48149 Münster, Germany

¹⁰SUBATECH, Ecole des Mines, Nantes, France

¹¹Gesellschaft für Schwerionenforschung (GSI), D-64220 Darmstadt, Germany

¹²Universiteit Utrecht/NIKHEF, NL-3508 TA Utrecht, The Netherlands

¹³University of Lund, SE-221 00 Lund, Sweden

¹⁴University of Tsukuba, Ibaraki 305, Japan

¹⁵Nuclear Physics Institute, CZ-250 68 Rez, Czech Republic

¹⁶KVI, University of Groningen, NL-9747 AA Groningen, The Netherlands

¹⁷Institute for Nuclear Studies, PL-00-681 Warsaw, Poland

¹⁸MIT, Cambridge, Massachusetts 02139

¹⁹Institute of Physics, 751 005 Bhubaneswar, India

²⁰University of Tennessee, Knoxville, Tennessee 37966

(Received 15 December 2000; published 31 May 2001)

Localized fluctuations in the multiplicity of charged particles and photons produced in central 158A GeV/c Pb+Pb collisions are studied. The charged versus neutral correlations in common $\eta-\phi$ phase space regions of varying azimuthal size are analyzed by two different methods. The analysis provides a model-independent demonstration of nonstatistical fluctuations in both charged particle and photon multiplicities in limited azimuthal regions. However, no correlated charge-neutral fluctuations are observed, contrary to expectations for the production of a disoriented chiral condensate. The result is not explained by the widely used VENUS model.

The formation of hot and dense matter in high energy heavy-ion collisions offers the possibility to create a new phase where matter is deconfined and chiral symmetry is restored. Indications for the formation of such a quark gluon plasma (QGP) phase are provided by several results from experiments at the CERN SPS [1]. Event-by-event fluctuations in the particle multiplicities and their ratios have recently been predicted to provide information about the nature of the QCD phase transition [2,3]. Fluctuations may also be caused by Bose-Einstein correlations, resonance decays, or more exotic phenomena such as pion lasers [4]. Enhanced fluctuations in neutral to charged pions have been predicted as a signature of the formation of disoriented chiral condensates (DCC) [5–8], which might be one of the most interesting predicted consequences of chiral symmetry restoration.

Theoretical predictions suggest that isospin fluctuations, caused by formation of a DCC, would produce clusters of coherent pions in localized phase space regions or domains. The probability distribution of the neutral pion fraction in such a domain would follow the relation $P(f) = 1/2 \sqrt{f}$, where $f = N_{\pi^0}/N_{\pi}$. Thus DCC formation in a given domain would be associated with large event-by-event fluctuations in the ratio of neutral to charged pions in that domain. Experimentally, such fluctuations can be deduced from the measurement of fluctuations in the number of photons to charged particles in limited $\eta - \phi$ regions. The anti-Centauro events, reported by the JACEE Collaboration [9], with large charged-neutral fluctuations are possible candidates for DCC events. The studies carried out so far in $p - \bar{p}$ [10] and heavy-ion [11,12] reactions have searched for fluctuations which extend over a large region of phase space. These measurements have provided upper limits on the presence of DCC-like fluctuations.

In this Rapid Communication we present first results on the search for nonstatistical event-by-event fluctuations in the relative number of charged particles and photons in localized $\eta - \phi$ phase space regions for central 158A GeV/c Pb+Pb collisions. The data presented here were taken with the 158A GeV Pb beam of the CERN SPS on a Pb target of 213 μm thickness during a period of WA98 operation without magnetic field. The analysis makes use of a subset of detectors of the WA98 experiment. Charged particle hits (N_{ch}) were counted using a circular silicon pad multiplicity detector (SPMD) [11] located 32.8 cm downstream from the target. It provided uniform pseudorapidity coverage in the region $2.35 < \eta < 3.75$. The detector was 99% efficient for charged particle detection. The photon multiplicity was measured using a preshower photon multiplicity detector (PMD) [13] placed 21.5 m downstream of the target and covering the pseudorapidity range $2.9 < \eta < 4.2$. Clusters of hit scintillator pads having total energy deposit above a hadron rejection threshold are identified as photonlike ($N_{\gamma\text{-like}}$). For this analysis the pseudorapidity region of common coverage of the SPMD and PMD was selected ($2.9 < \eta < 3.75$). The acceptance in terms of transverse momentum (p_T) extends down to 30 MeV/c, although no explicit p_T selection is applied. Strict data selection and cleanup cuts have been applied as described in Refs. [11,14]. After cuts, a total of 85 K

central events, corresponding to the top 5% of the minimum bias cross section as determined from the measured total transverse energy, have been analyzed. Average multiplicities of $\langle N_{\text{ch}} \rangle = 323.8$ and $\langle N_{\gamma\text{-like}} \rangle = 335.7$ are obtained for this centrality selection.

The measured results are interpreted by comparison with simulated events and with several types of mixed events. Simulated events were generated using the VENUS 4.12 [15] event generator with default parameters. The output was processed through a WA98 detector simulation package in the GEANT 3.21 [16] framework. The centrality selection for the simulated data has been made in a manner identical to the experimental data by selection on the simulated total transverse energy in the WA98 acceptance ($3.2 < \eta < 5.4$). The simulated VENUS+GEANT events (referred as V+G) were then processed with the same analysis codes as used for the analysis of the experimental data. The photon counting efficiency and the purity of the γ -like sample were determined from these simulations to be 68% and 65%, respectively, for central events [14].

The effect of nonstatistical DCC-like charged-neutral fluctuations has been studied within the framework of a simple model in which the output of the VENUS event generator has been modified. To implement the DCC effect, the charges of the pions within a localized $\eta - \phi$ region from VENUS are interchanged pairwise ($\pi^+ \pi^- \leftrightarrow \pi^0 \pi^0$) according to the $P(f) = 1/2 \sqrt{f}$ probability distribution. The DCC-like fluctuations were generated over $\eta = 3 - 4$ for varying intervals in $\Delta\phi$. Since the probability to produce events with DCC domains is unknown, ensembles of events, here referred to as “nDCC events,” were produced as a mixture of normal events with varying fractions of pure DCC-like events. The nDCC events were then tracked through GEANT.

In the search for evidence of nonstatistical charged-neutral fluctuations, two different analysis techniques have been applied. The first method employed in the present analysis is the technique of discrete wavelet transformations (DWT). DWT methods are now widely used in many applications, such as data compression and image processing, and have been shown to provide a powerful means to search for localized domains of DCC [17,18]. While there are several families of wavelet bases distinguished by the number of coefficients and the level of iteration, we have used the frequently employed $D - 4$ wavelet basis [20]. The analysis has been performed with the sample function chosen to be the photon fraction, given by $f'(\phi) = N_{\gamma\text{-like}}(\phi) / (N_{\gamma\text{-like}}(\phi) + N_{\text{ch}}(\phi))$ as a function of the azimuthal angle ϕ , with highest resolution scale $j_{\text{max}} = 5$. The input to the DWT analysis is the spectrum of the sample function at the smallest bin size corresponding to the highest resolution scale, j_{max} , where the number of bins is $2^{j_{\text{max}}}$. The sample function is then analyzed at different scales j by being rebinned into 2^j bins. The DWT analysis yields a set of wavelets or father function coefficients (FFC) at each scale from $j = 1$ to $(j_{\text{max}} - 1)$. The coefficients obtained at a given scale, j , are derived from the distribution of the sample function at one higher scale, $j + 1$. The FFCs quantify the deviation of the bin-to-bin fluctuations in the sample function at that higher scale relative to the average behavior. The presence of localized nonstatistical

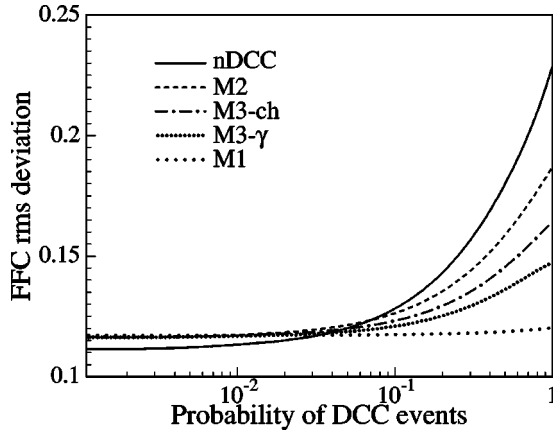


FIG. 1. The rms deviations of the FFC distributions at $j=1$ for simulated nDCC events with extent $\Delta\phi_{\text{DCC}}=90^\circ$ and for various mixed events constructed from those events, as a function of the fraction of DCC-like events present in the nDCC sample.

fluctuations will increase the root mean square (rms) deviation of the distribution of FFCs and may result in non-Gaussian tails [17,18].

The sensitivity of the DWT technique as used in this analysis is demonstrated in Fig. 1 where it has been applied to the simulated nDCC events. The rms deviation of the FFC distribution is shown as a function of the fraction of DCC-like events in the nDCC sample. The rms deviation is observed to increase strongly with increasing DCC-like fraction. Due to the inherent uncertainties in the description of ‘‘normal’’ physics and detector response in the V+G simulations, the observation of an experimental result with rms which differs from simulation with zero DCC fraction cannot be taken alone as evidence of DCC observation. For this reason four different types of mixed events have been created from the real or simulated events in order to search for nonstatistical fluctuations by removing various correlations in a controlled manner while preserving the characteristics of the measured distributions as accurately as possible. The first type of mixed events (M1) are generated by mixing hits in both the PMD and SPMD separately, with no two hits taken from the same event. Hits within a detector in the mixed events are not allowed to lie within the two track resolution of that detector. The second kind of mixed events (M2) are generated by mixing the unaltered PMD hits of one event with the unaltered SPMD hits of a different event. Intermediate between the M1 and M2 kinds of mixed events is the case where the hits within the PMD are unaltered while the SPMD hits are mixed (M3- γ), or the SPMD hits are unaltered while the PMD hits are mixed (M3-ch). In each type of mixed event the global (bin 1) $N_{\gamma\text{-like}}-N_{\text{ch}}$ correlation is maintained as in the real event.

The rms deviations of the FFCs for the different kinds of mixed events produced from the nDCC events are also shown in Fig. 1. In the case of vanishing DCC-like fluctuations, the rms values of the various types of mixed events are very close to each other, and higher than the V+G rms values. This is due to the presence of additional correlations between N_{ch} and $N_{\gamma\text{-like}}$, mostly as a result of the charged particle contamination in the $N_{\gamma\text{-like}}$ sample. The rms devia-

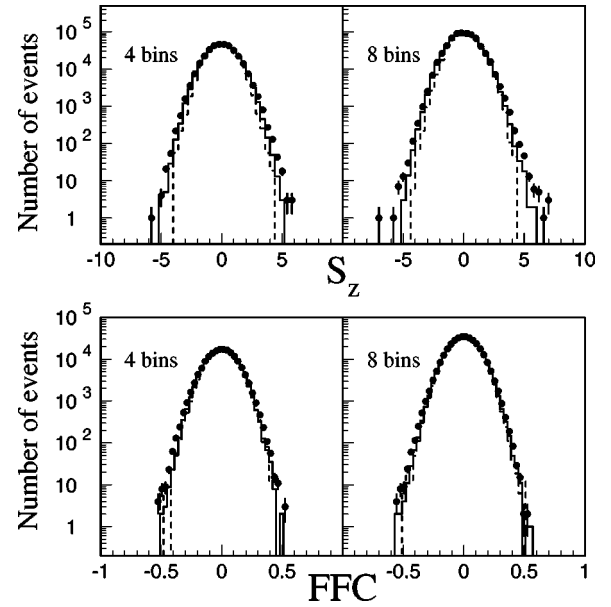


FIG. 2. The S_z and FFC distributions for four and eight divisions in ϕ . The experimental data, M1, and V+G events are shown by solid circles, solid and dashed histograms, respectively. The number of data and mixed events is the same. The distribution for the V+G events is normalized to the data.

tions for the M1 events are found to be almost independent of probability of DCC-like events, while the rms deviations of the M2 events increase similarly, but more weakly, than those of the nDCC events. The rms deviations for the M3 sets of events are found to lie between M2 and M1. Thus, the sequence of the mixed events relative to the simulated events (or data) gives a model independent indication of the presence and source of nonstatistical fluctuations. The simple DCC model used here results in an anticorrelation between $N_{\gamma\text{-like}}$ and N_{ch} . It also results in nonstatistical fluctuations in both $N_{\gamma\text{-like}}$ and N_{ch} . It is seen that the M2 events have only the $N_{\gamma\text{-like}}-N_{\text{ch}}$ anticorrelation removed while the M1 events have all nonstatistical fluctuations and correlations removed. The M3 mixed events give intermediate results because they contain only the $N_{\gamma\text{-like}}$ (M3- γ) or N_{ch} (M3-ch) nonstatistical fluctuations.

The FFC distributions extracted from the measured $f'(\phi)$ ratio are shown in the bottom panel of Fig. 2 for the experimental data, for M1 events (from data), and for V+G events. The results are shown for scales $j=1$ and 2, which carry information about fluctuations at 90° and 45° in ϕ . The FFC distributions of the experimental distributions are seen to be broader than the V+G and M1 results. This suggests the presence of nonstatistical fluctuations.

A more conventional method similar to that described in Ref. [11] has also been used to search for nonstatistical fluctuations. The correlation between $N_{\gamma\text{-like}}$ and N_{ch} has been studied in varying ϕ intervals, by dividing the entire ϕ space into two, four, eight, and 16 bins. The correlation plot of N_{ch} versus $N_{\gamma\text{-like}}$ [19] is obtained for each ϕ segmentation, and fitted to a second order polynomial to obtain a correlation axis (Z). The distance of separation (D_z) between the data points and the Z axis has been calculated with the convention

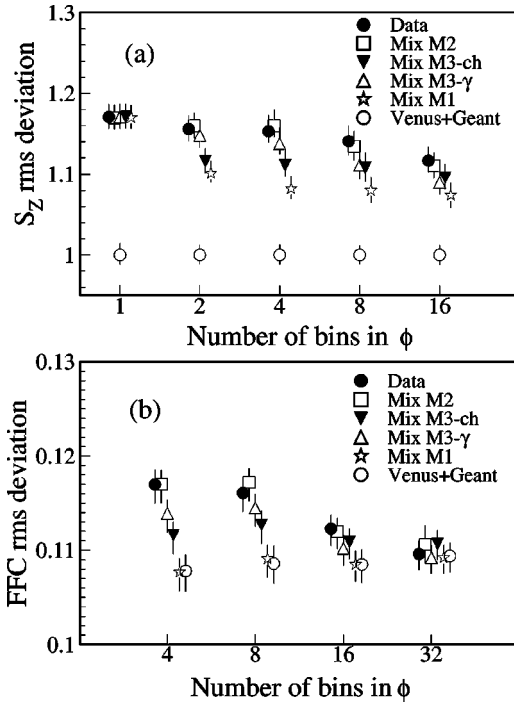


FIG. 3. The rms deviations of the S_Z and FFC distributions for various divisions in the azimuthal angle. For V+G $s(D_Z)=17.2, 11.8, 8.12, 5.66,$ and 4.01 for one to 16 bins, respectively.

that D_Z is positive for points below the Z axis (increasing $N_{\gamma\text{-like}}$). In order to compare fluctuations at different bin sizes having different multiplicities we use a scaled variable, $S_Z = D_Z/s(D_Z)$, where $s(D_Z)$ is the rms deviation of the D_Z distributions for V+G events. The presence of events with localized nonstatistical fluctuations would be expected to result in a broader distribution of S_Z compared to those for normal events. The S_Z distributions calculated at four and eight bins in ϕ angle are shown in the top panel of Fig. 2 for data, M1, and V+G events. The experimental distributions are broader than the simulation and M1 results, again indicating the presence of additional fluctuations.

The rms deviations of the S_Z and FFC distributions as a function of the number of bins in azimuth is shown for experimental data, mixed events, and V+G in Fig. 3. As noted in the discussion of Fig. 1, even in the absence of DCCs there exist uninteresting correlations between $N_{\gamma\text{-like}}$ and N_{ch} which are removed by the event mixing procedure and thereby result in a difference between the real and mixed events. The mixed event rms values of Fig. 3 have therefore been rescaled by the percentage difference between the rms deviations of the V+G distributions and those of the corresponding V+G mixed events in order to better illustrate effects in the data beyond those present in V+G. The statistical errors on the values are small and lie within the size of the symbols. The error bars include both statistical and systematic errors. The systematic errors have been estimated by investigation of effects such as the uncertainties in the detection efficiencies, gain fluctuations, backgrounds, binning variations, and fitting procedures. The total systematic error

was obtained as the sum in quadrature of the individual error contributions which have been determined from the variation of the final result according to the maximum estimated uncertainty for each effect.

Since the mixed events are constructed to maintain the $N_{\gamma\text{-like}} - N_{\text{ch}}$ correlations for the full azimuth (bin 1), the rms deviations of data and mixed events for this bin are identical. The difference of the S_Z rms deviations between data and V+G for this bin is the same as reported in an earlier WA98 publication [11]. The comparison of V+G and the M1 mixed events demonstrates the utility of the DWT method to normalize out the average behavior when the bin-to-bin fluctuation information is extracted. For two, four, and eight bins the values of the S_Z rms deviations of the data are 2.5σ , 3.0σ , and 2.4σ larger than those of M1 events, respectively, where $\sigma = \sqrt{(\sigma_{\text{lower}}^{\text{data}})^2 + (\sigma_{\text{upper}}^{\text{M1}})^2}$ is the sum in quadrature of the total error separating the points. Similarly, the FFC rms deviations at four and eight bins for data are 3.7σ and 2.8σ larger than those of the M1 events. At 16 and 32 bins, the result for mixed events and data agree within the quoted errors. The rms deviations of the M2 events agree with those of the experimental data within error for all bins. The M3-type mixed events are found to be similar to each other within the quoted errors and lie between M1 and M2.

The observation that the rms deviations of the S_Z and FFC distributions for experimental data are larger than those of the M1 events provides model-independent evidence for the presence of localized nonstatistical fluctuations. However, the comparison of the rms deviations for data with those of M2 events implies the absence of event-by-event correlated fluctuations in $N_{\gamma\text{-like}}$ versus N_{ch} . The M3-type mixed events indicate the presence of localized independent fluctuations in $N_{\gamma\text{-like}}$ and N_{ch} of similar magnitude.

If the amount of DCC-like fluctuations in the experimental data were large, then the rms deviations shown in Fig. 3 for data would have been larger compared to those of M2 events. Since this is not the case, we compare the measured results with those obtained from the simulation as shown in Fig. 1 to extract upper limits on the probability of DCC-like fluctuations at the 90% confidence level. Within the context of this simple DCC model, upper limits on the presence of localized nonstatistical DCC-like fluctuations of 10^{-2} for $\Delta\phi$ between 45° – 90° and 3×10^{-3} for $\Delta\phi$ between 90° – 135° are extracted.

In summary, a detailed event-by-event analysis of the fluctuations in the $\eta - \phi$ phase space distributions of charged particles and photons has been performed for central Pb+Pb collisions at 158A GeV using two complementary analysis methods. The first analysis employed the discrete wavelet transformation technique to investigate the relative magnitude of the $N_{\gamma\text{-like}}/(N_{\text{ch}} + N_{\gamma\text{-like}})$ fluctuations in adjacent ϕ intervals of varying size. The second method studied the magnitude of the $N_{\gamma\text{-like}}$ versus N_{ch} multiplicity fluctuations in decreasing ϕ regions. Both analysis methods provide model-independent evidence for nonstatistical fluctuations at the 3σ level for ϕ intervals of greater than 45° . This is shown to be due to nonstatistical fluctuations in both $N_{\gamma\text{-like}}$ and N_{ch} . However, no significant correlated fluctuations in

$N_{\gamma\text{-like}}$ versus N_{ch} were observed, contrary to naive expectations for a DCC effect. The result is not explained by VENUS+GEANT simulations or by a simple model of DCC-like fluctuations. The interpretation of the result remains an open question.

We wish to express our gratitude to the CERN accelerator division for the excellent performance of the SPS accelerator complex. We acknowledge with appreciation the effort of all engineers, technicians, and support staff who have participated in the construction of this experiment. This work was supported jointly by the German BMBF and DFG, the U.S. DOE, the Swedish NFR and FRN, the Dutch Stichting FOM,

the Polish KBN under Contract No. 621/E-78/SPUB/CERN/P-03/DZ211, the Grant Agency of the Czech Republic under Contract No. 202/95/0217, the DAE, DST, CSIR, and UGC of the Government of India, the Indo-FRG Exchange Program, the PPE division of CERN, the Swiss National Fund, the INTAS under Contract No. INTAS-97-0158, ORISE, the University of Tsukuba Special Research Projects, and the JSPS. ORNL is managed by UT-Battelle, LLC, for the U.S. Department of Energy under Contract No. DE-AC05-00OR22725. The MIT group has been supported by the U.S. Department of Energy under Cooperative Agreement No. DE-FC02-94ER40818.

-
- [1] *Proceedings of Quark Matter '99* [Nucl. Phys. **A661** (1999)].
 [2] M. Stephanov *et al.*, Phys. Rev. Lett. **81**, 4816 (1998).
 [3] M. Asakawa, U. Heinz, and B. Müller, Phys. Rev. Lett. **85**, 2072 (2000); S. Jeon and V. Koch, *ibid.* **85**, 2076 (2000).
 [4] S. Pratt, Phys. Lett. B **301**, 159 (1993).
 [5] A. A. Anselm and M. G. Ryskin, Phys. Lett. B **266**, 482 (1991).
 [6] J. D. Bjorken, Int. J. Mod. Phys. A **7**, 4189 (1992).
 [7] J.-P. Blaizot and A. Krzywicki, Phys. Rev. D **46**, 246 (1992).
 [8] K. Rajagopal and F. Wilczek, Nucl. Phys. **B399**, 395 (1993); **B404**, 577 (1993). S. Gavin *et al.*, Phys. Rev. Lett. **72**, 2143 (1994).
 [9] JACEE Collaboration, C. M. G. Lattes *et al.*, Phys. Rep. **65**, 151 (1980).
 [10] Minimax Collaboration, T. C. Brooks *et al.*, Phys. Rev. D **61**, 032003 (2000).
 [11] WA98 Collaboration, M. M. Aggarwal *et al.*, Phys. Lett. B **420**, 169 (1998).
 [12] NA49 Collaboration, H. Appelshauser *et al.*, Phys. Lett. B **459**, 679 (1999).
 [13] M. M. Aggarwal *et al.*, Nucl. Instrum. Methods Phys. Res. A **424**, 395 (1999).
 [14] WA98 Collaboration, M. M. Aggarwal *et al.*, Phys. Lett. B **458**, 422 (1999).
 [15] K. Werner, Phys. Rep. **232**, 87 (1993).
 [16] R. Brun *et al.*, GEANT3 guide, CERN/DD/EE/84-1, 1984.
 [17] Z. Huang *et al.*, Phys. Rev. D **54**, 750 (1996).
 [18] B. K. Nandi *et al.*, Phys. Lett. B **461**, 142 (1999).
 [19] WA98 Collaboration, B. Mohanty *et al.*, Czech. J. Phys. **50**, 126 (2000).
 [20] *Numerical Recipes* (Cambridge University Press, Cambridge, 1998).